Stand Structure and Recent Climate Change Constrain Stand Basal Area Change in European Forests: A Comparison Across Boreal, Temperate, and Mediterranean Biomes

8 authors, including:

Paloma Ruiz-Benito
University of Acalá
72 PUBLICATIONS   1,054 CITATIONS

SEE PROFILE

Jaime Madrigal-González
Institute for Environmental Sciences, University of Geneva
52 PUBLICATIONS   369 CITATIONS

SEE PROFILE

Sophia Ratcliffe
National Bioversity Network Trust
34 PUBLICATIONS   488 CITATIONS

SEE PROFILE

David Coomes
University of Cambridge
267 PUBLICATIONS   13,668 CITATIONS

SEE PROFILE

Some of the authors of this publication are also working on these related projects:

The role of tree species composition and forest structure on cooling as forest ecosystem service provision View project

PN-II-ID-PCE-2011-3-0781 Forest GHG Management View project

ECOSYSTEMS Springer

Stand structure and recent climate change constrain stand basal area change in European forests: a comparison across boreal, temperate and Mediterranean biomes

SCHOLARONE™
Manuscripts

1 **Stand structure and recent climate change constrain stand basal area change in**

2 **European forests: a comparison across boreal, temperate and Mediterranean**

3 **biomes**

4 **Short title:** Drivers of basal area change across Europe

5 **P. Ruiz-Benito[1,2,3]*, J. Madrigal-González[2]** (ecojmg@hotmail.com)**, S. Ratcliffe[4]**

6 (sophia.ratcliffe@uni-leipzig.de)**, D. A. Coomes[5]** (dac18@cam.ac.uk)**, G. Kändler[6]**

7 (Gerald.Kaendler@forst.bwl.de)**, A. Lehtonen[7]** (aleksi.lehtonen@metla.fi)**, C. Wirth[4,8]**

8 (cwirth@uni-leipzig.de)**, M. A. Zavala[2]** (madezavala@gmail.com)**,**

9 [1]*Department of Forest Ecology and Genetics, ForestResearch Center - Instituto Nacional de*
10 *Investigación y Tecnología Agraria y Alimentaria (CIFOR-INIA), Ctra. de la Coruña, Km. 7,5.*
11 *28040. Madrid, Spain.*

12 [2]*Forest Ecology and Restoration Group, Department of Life Sciences, Science Building,*
13 *University of Alcala, Campus Universitario, 28871, Alcalá de Henares (Madrid), Spain.*

14 [3]*Biological and Environmental Sciences, School of Natural Sciences.University of Stirling. FK9*
15 *4LA, Stirling, United Kingdom.*

16 [4]*University of Leipzig. AG Spezielle Botanik und Funktionelle Biodiversität. Johannisallee 21-2.*
17 *04103 Leipzig, Germany.*

18 [5]*Forest Ecology and Conservation Group, Department of Plant Sciences, University of*
19 *Cambridge, Downing Street, Cambridge, CB3 2EA, UK.*

20 [6]*The Forest Research Institute, Wonnhaldestr. 4. 79100 Freiburg, Germany.*

21 [7]*Finnish Forest Research Institute, Vantaa Research Centre, PO Box 18, 01301 Vantaa,*
22 *Finland.*

23 [8]*German Centre for Integrative Biodiversity Research (iDiv) Halle-Jena-Leipzig, Deutscher*
24 *Platz 5e, 04103 Leipzig, Germany.*

25 **Correspondence:** Paloma Ruiz Benito. *E-mail: palomaruizbenito@gmail.es. Phone: 00 34 637*
26 *19 43 53. Fax: 00 34 91 357 22 93.*

27 **Type of paper:** Original Article

28   **Authorship**: JM, PRB and MAZ conceived the design; DC, GK, AL, SR, PRB, CW and MAZ

29   collected the data; JM, PRB and SR analyzed data; DC, JM, SR and PRB contributed to the

30   methods, and all the authors wrote the article.

31

32 **ABSTRACT**

33   European forests have a prominent role in the global carbon cycle and an increase in

34   carbon storage has been consistently reported during the 20th century. Any further

35   increase in forest carbon storage, however, could be hampered by increases in aridity

36   and extreme climatic events. Here we use forest inventory data to identify the relative

37   importance of stand structure (stand basal area and mean d.b.h.), mean climate (water

38   availability) and recent climate change (temperature and precipitation anomalies) on

39   forest basal area change during the late 20th century in three major European biomes.

40   Using linear mixed-effects models we observed that stand structure, mean climate and

41   recent climatic change strongly interact to modulate basal area change. Although we

42   observed a net increment in stand basal area during the late 20th century, we found the

43   highest basal area increments in forests with medium stand basal areas and small to

44   medium sized trees. Stand basal area increases correlated positively with water

45   availability, and were enhanced in warmer areas. Recent climatic warming caused an

46   increase in stand basal area, but this increase was offset by water availability. Based on

47   recent trends in basal area change we conclude that the potential rate of aboveground

48   carbon accumulation in European forests strongly depends on both stand structure and

49   concomitant climate warming, adding weight to suggestions that European carbon

50   stocks may saturate in the near future.

51   **Keywords**: carbon sink, climatic variability, competition, inventory-based data,

52   minimum temperature, mixed models, water availability, stand basal area change.

53   **INTRODUCTION**

54   Forests cover more than 30% of the global land surfaces (FRA, 2010), store large

55   reservoirs of carbon (Goodale and others 2002; Pan and others 2011), harbour around

56   two thirds of terrestrial biodiversity (Millennium Ecosystem Assessment 2005) and

57   promote multiple ecosystem services (Gamfeldt and others 2013). Forests play a central

58   role in the global carbon cycle, but the factors controlling terrestrial carbon exchanges

59   and their magnitude remain controversial (Valentini and others 2000; Nabuurs and

60   others 2003; Bellassen and Luyssaert 2014). For example, it is widely accepted that

61   current increases in forest biomass observed in many temperate forests result partially

62   from positive effects of global change (e.g. Pastor and Post 1988; Nabuurs and others

63   2003; Ciais and others 2008; Hember and others 2012; Peng and others 2014) and

64   changes in forest management regimes (e.g. Spiecker 1999; Luyssaert and others 2010),

65   but the influences of climate change and extreme climatic events on biomass changes

66   are not well understood (Dixon and others 1994; Schimel 2007; McMahon and others

67   2010).

68   Future forest carbon sinks could be affected by large-scale changes in mortality

69   and growth rates, both of which are related to climate, forest structure and the

70   interactions between these factors (e.g. van Mantgem and others 2009; Dietze and

71   Moorcroft 2011; Ruiz-Benito and others 2013). The rate of increase in carbon storage

72   depends on forest structure, climate warming, CO_2 fertilisation and nitrogen deposition

73   effects (Nabuurs and others 2003; Ciais and others 2008; Pan and others 2011).

74   Although the magnitude of these effects remains uncertain, it has been shown that

75   recent climate change and CO_2 fertilisation could have a positive impact on tree growth

76   (Cao and Woodward 1998; Ciais and others 2008; Bellassen and others 2011).

77   However, these positive effects could be overwhelmed by the effects of increased

78   climatic variability and extreme climatic events, such as more frequent and more intense

79   drought events (e.g. Ciais and others 2005; Zhao and Running 2010; Hoch and Körner

80   2012). Moreover, regional studies have not shown consistent trends in forest growth

81   rates; growth is increasing in temperate areas but no clear trends have been found in

82   European boreal or Mediterranean forests (Spiecker, 1999). On the other hand, recent

83   worldwide episodes of increased defoliation and tree mortality have been related to

84   climate-induced processes (Allen and others 2010; Carnicer and others 2011). Forest

85   carbon sinks could be potentially affected by large-scale changes in mortality and

86   growth rates, both of which have been related to climate and/or its interaction with

87   forest structure (e.g. van Mantgem and others 2009; Dietze and Moorcroft 2011; Ruiz-

88   Benito and others 2013).

89   European forests have been globally important carbon sinks (Ciais and others

90   2008; Nabuurs and others 2003), but what will happen in future is a matter of intense

91   debate (Narbuurs and others 2013). As a result of climate change, mean temperatures

92   are likely to increase, with northern Europe experiencing warmer winters and

93   Mediterranean regions warmer summers (Christensen and others 2007). Meanwhile,

94   climate change scenarios suggest that precipitation could increase in northern Europe

95   and decrease in Mediterranean regions (Christensen and others 2007). The exposure of

96   Mediterranean systems to even hotter, drier summers could result in the death of trees

97   normally regarded as drought tolerant, because the combination of low soil moisture

98   potentials and strong vapour pressure deficits push water transport systems to their limit

99   (Allen and others 2010; Ruiz-Benito and others 2013). Thus, climate change could

100   result in a reduction of carbon gains in the water-limited forests of Europe (Vayreda and

101   others 2012), that could even counteract gains arising from the abandonment of

102   agricultural lands (Canadell and Raupach 2008).

103   Understanding how forest structure and climate interact to drive biomass change

104 across European forests, from boreal to temperate and Mediterranean forests is critical

105 to infer future trends in forest carbon sinks. The role of European forests in the global

106 carbon cycle in the second half of the 20th century has been largely estimated through

107 inventory-based national statistics (e.g. Goodale and others 2002; Nabuurs and others

108 2003; Ciais and others 2008; Bellassen and others 2011). Recently tree level

109 information from consecutive inventories has become available in a growing number of

110 EU countries, allowing us to better estimate large-scale demographic processes (e.g.

111 Kunstler and others 2011; Benito-Garzón and others 2013; García-Valdés and others

112 2013, Vilà and others 2013). In this study we performed, for the first time, a large-scale

113 analysis of the main patterns and drivers of recent stand basal area change in the three

114 main biomes of European forests, using plot-level forest inventory information. Our

115 specific objectives were: (i) to examine recent decadal patterns of forest basal area

116 change, growth and mortality across Mediterranean, temperate and boreal biomes in

117 Europe; and (ii) to quantify the effect of stand structure, mean climate and recent

118 climate change on stand basal area change.

119 **MATERIAL AND METHODS**

120 **Data of stand basal area change and its components**

121 We compiled information from consecutive National Forest Inventories (NFI hereafter)

122 of Spain, Germany and Finland (see methodological details in Appendix 1 of

123 supplementary material), which encompass stands belonging to Mediterranean,

124 temperate and boreal biomes (Figure 1a). We selected plots from consecutive surveys

125 where tree-level data on ingrowth, surviving and dead trees was recorded in both

126 surveys (see supplementary Appendix 1 and Table S1).

127   From the initial plots of the three NFIs we selected a total of 40,521 plots where

128   at least one adult tree was measured (i.e. d.b.h. > 10 cm) and where there was no

129   evidence of thinning or harvesting in either of the two consecutive surveys. Plots with

130   any sign of harvesting were excluded for two reasons: (i) biomass loss due to harvesting

131   implies an assessment of growth considering only surviving trees, which could result in

132   biased estimates of real productivity in natural forests–; and (ii) harvesting usually

133   triggers an immediate growth release in neighbouring trees and, therefore, management

134   could affect carbon stock changes (Vayreda and others 2012).

135   In the 40,521 plots each tree alive in the first inventory was recorded as either

136   alive or dead in the second inventory. We estimated the absolute change in basal area

137   and the relative growth and mortality rates in each plot. Thus, we calculated: (i) stand

138   basal area change (m^2 ha^{-1} yr^{-1}, SBAc hereafter) as the difference in stand basal area

139   between the two surveys with respect to the time interval; (ii) basal area growth rate

140   (annual percentage, SBA_{gain}) as the sum of basal area increments of all live trees present

141   in each survey with respect to the time interval and initial stand basal area; and (iii)

142   basal area loss rate due to natural mortality (annual percentage, SBA_{loss}) as the basal

143   area lost between consecutive surveys due to mortality, again with respect to the initial

144   stand basal area and time interval following Sheil and others (1995). Basal area loss rate

145   was greater than zero in 25.4% of the plots included in this analysis (i.e. from the

146   40,521 measured plots included in this analysis 10,303 had a basal area loss rate greater

147   than zero). We used stand basal area change instead of biomass change directly because:

148   (i) basal area has been identified as reliable a proxy for biomass (e.g. Slik and others

149   2010); (ii) allometric equations do not exist for all 158 species present in the 40,521

150   plots included in the analysis; and (iii) allometric relationships can vary along the large

151   climatic gradient covered in this study (e.g. Lines and others 2012). We produced maps

152 of SBAc, SBA$_{gain}$ and SBA$_{loss}$ using ArcGIS 10 (ESRI Inc., Redlands, CA, USA; Figure

153 1).

Forest structure and climate data

155 We used two forest structure variables, two climatic variables and two variables

156 representative of recent climatic change as potential predictors of recent stand basal area

157 changes. Mean tree diameter (d_m, mm) and stand basal area (BA, m^2 ha^{-1}), in the first

158 survey, were used to represent forest structure.

159 To characterise the spatial variability of climate across the three biomes, for each

160 of the plots we obtained climatic variables from WorldClim (Hijmansand others 2005)

161 and CGIAR-CSI GeoPortal, using CGIAR-CSI Global-Aridity and Global-PET

162 Database (Zomer and others 2007; 2008). Two climatic variables were selected to

163 characterise the climate in each plot (see details of variable selection in supplementary

164 Appendix 2 and Table S2): an index of water availability (WAI) and mean temperature

165 of the coldest quarter (hereafter minimum temperature, Tmin) (based on data between

166 1950 and 2000). WAI integrates temperature and rainfall in each plot (i.e. annual

167 precipitation   minus   potential   evapotranspiration   divided   by   potential

168 evapotranspiration). Negative values of WAI correspond to dry areas and positive

169 values to wet areas, and it has been shown to be an important driver of tree carbon

170 storage in the Mediterranean region (Vayreda and others 2012). Minimum temperature

171 is thought to be an important constraint in eastern European limits of tree species

172 distribution (e.g. Sykes and Prentice 1996).

173 The magnitude of recent climate change was quantified by comparing mean

174 annual temperature and precipitation over the study period with the mean of each

175 climatic variable over the reference period 1900-2006, using mean monthly climate data

176   at 0.5 x 0.5 degree resolution from UDel_AirT_Precip data provided by the

177   NOAA/OAR/ESRL PSD (Boulder, Colorado, USA). The study period was defined as

178   the number of years between the two consecutive inventories plus two years before the

179   first survey (i.e. 1984-2006 Spain; 1984-2002 Germany; 1983-1995 Finland) to include

180   lagged effects of climate on growth or mortality (Vayreda and others 2012). We

181   calculated absolute temperature anomalies and relative precipitation anomalies, using

182   yearly averages calculated using mean monthly climate data (i.e. from January to

183   December). The absolute temperature anomaly (ºC) was defined as the difference

184   between the mean temperature for the study period and the mean value for the reference

185   period (1900-2006). The relative precipitation anomaly (%) was defined as the ratio

186   between the equivalent differences for precipitation and the mean value for precipitation

187   for the reference period. The absolute temperature anomalies varied from -0.3 to 1 ºC

188   among grid cells (with an average increment of 0.46 ºC), while the relative precipitation

189   anomalies varied from -18.7% to 14.6% (with an average of -2.5%, see supplementary

190   Figure S1 and S2).

Statistical analyses

192   We modelled stand basal area change (SBAc, m^2 ha^{-1} yr^{-1}) using linear mixed-

193   effects models, with a Gaussian distribution of residuals and used an identity link for the

194   response variable. All analyses were performed in R version 2.15.1 (R Core Team

195   2012), using the "lme4" package (Bates and others 2012).

196   The six fixed predictor variables of SBAc used were: stand basal area (BA,

197   m^2/ha), mean d.b.h. (d_m, mm), water availability (WAI, %), minimum temperature

198   (Tmin, ºC), absolute temperature anomaly (TA, ºC) and relative precipitation anomaly

199   (PA, %) (see mean values in supplementary Figure S3 and Table S3). Due to the

200   clustered nature of the sampling in Finland and Germany (where plots are aggregated in

201   groups of four; see Appendix 1 for more information), we included cluster as a random

202   effect in the model. We fitted country as a fixed effect because it only has three levels,

203   and as such is inappropriate as a random effect (see Bolker and others 2009). Our full

204   model also included as fixed effects linear and quadratic terms for each explanatory

205   variable. Based on our initial hypothesis we also included pair-wise interactions

206   between stand structure and climate variables: $d_m \times BA$, $WAI \times Tmin$, $BA \times WAI$, $BA \times$

207   $Tmin$, $BA \times TT$, $BA \times PT$, $d_m \times WAI$, $d_m \times Tmin$, $d_m \times TT$, $d_m \times PT$ and $WAI \times TT$, WAI

208   $\times PT$ and $Tmin \times TT$. All the numerical predictor variables were standardised (i.e. the

209   mean was subtracted from each value and divided by the standard deviation), enabling

210   the interactions to be included in the model (Zuur and others 2009). Additionally, in

211   order to detect colinearity between explanatory variables, we calculated the variance

212   inflation factors (VIFs) for each predictor variable. VIFs calculate the degree to which

213   collinearity inflates the estimated regression coefficients as compared with the

214   orthogonal predictors (Belsey, 1991; Oksanen and others 2010). Our results confirmed

215   that collinearity was not a major problem in our data (VIF < 3).

216   The most parsimonious model was determined using BIC (Bayesian Information

217   Criterion) as an indicator of both parsimony and likelihood (Burnham and Anderson

218   2002). To identify the best-supported model we first constructed candidate models in

219   which each of the interactions were dropped and if the difference in BIC between the

220   reduced and full models was less than two then the simpler model was selected (Hilborn

221   and Mangel 1997; Pinheiro and Bates 2000). The process was then repeated for all the

222   independent variables this time comparing each individual predictor variable with a

223   model containing all response variables without any interactions, using the differences

224   in BIC to quantify the relative importance of each predictor variable. Finally, parameter

225   estimates and confidence intervals of the best-supported model were obtained using

226   restricted maximum likelihood (REML), which minimizes the likelihood of the

227   residuals from the fixed-effect portions of the model (Zuur and others 2009).

228   The marginal R^2 (proportion of variance explained by fixed factors) and

229   conditional R^2 (proportion of variance explained by both the fixed and random factors)

230   were estimated following Nakagawa and Schielzeth (2013). The parameter estimates

231   provide the basis for determining the magnitude of the effect of a given process, with

232   maximum likelihood estimates of parameter values close to zero indicating no effect.

233   Mean parameter estimates and 95% confidence intervals for the fixed effects were

234   estimated using bootstrapping methods available in the lme4 package (Bates and others

235   2012).

236   Response curves for each explanatory variable (varying between the 99%

237   percentiles observed in the data) were computed using the best supported model, fixing

238   the values of the other continuous variables at the observed mean (Table 1), and the

239   categorical variables to zero (i.e. the fixed country effect, Eq. (1)). Approximate

240   confidence intervals of the prediction were calculated from the variance-covariance

241   matrix of the fixed effects (± 2 × standard error of prediction). Response curves were

242   also computed with two variables varying between the 99% percentiles observed in the

243   data, with the rest held constant to the mean; these were visualised using three-

244   dimensional graphs.

245   **RESULTS**

246   **Patterns of stand basal area change and its components**

247   During the late 20th century there were positive mean stand basal area changes (SBAc)

248   in the Mediterranean, temperate and boreal biomes (Table 1, supplementary Table S3),

249   confirming that forests in these regions were accumulating basal area at a mean relative

250   annual rate of 3.82%. We observed the largest mean SBAc, growth and loss rates in the

251   temperate biome (Table 1, Figure 1b-d), with the highest basal area loss rates occurring

252   in Spanish temperate forests (i.e. Northern Iberian Peninsula, see Figure 1d and

253   supplementary Table S3). Forests with negative or near-zero SBAc were mainly

254   concentrated in the Mediterranean and northern boreal regions (Table 1, Figure 1b).

255   There was a positive correlation between SBAc and relative basal area gains due to

256   growth ($r = 0.41$, $P < 0.001$, Figure 1b,c), but SBAc was also affected by natural

257   mortality as it can be observed by the negative correlation between SBAc and basal area

258   loss ($r = -0.26$, $P < 0.001$, Figure 1b,d).

259   A latitudinal gradient in water availability (WAI) and minimum temperature was

260   observed (supplementary Figure S1). The Mediterranean biome had the driest areas (i.e.

261   negative WAI) with increasing water availability towards the temperate and boreal

262   biomes (Table 1), and minimum temperatures were lowest in the boreal biomes (Table

263   1). Regarding climatic anomalies in the late 20th century, the largest temperature

264   increments and precipitation reductions tended to be concentrated in Mediterranean and

265   cool temperate biomes (Table 1 and supplementary Figure S1).

266   **Effects of stand structure, climate and recent climate change on basal**

267   **area change**

268   The best-supported model included the effects of all predictor variables (marginal $R^2 =$

269   0.2743, conditional $R^2 = 0.3761$) and took the following functional form:

270

271    $SBAc = \underline{\beta_1} + \underline{\beta_2}(BA) + \underline{\beta_3}(BA^2) + \underline{\beta_4}(d_m) + (\underline{\beta_5}(d_m{}^2) + \underline{\beta_6}(WAI) + \underline{\beta_7}(Tmin) +$

272    $\underline{\beta_8}(Tmin^2) + \underline{\beta_9}(TA) + \underline{\beta_{10}}(PA) + (\underline{\beta_{11}}PA^2) + \underline{\beta_{12}}(SP) + \underline{\beta_{13}}(FI) + \underline{\beta_{14}}(BA)(d_m) +$

273    $\underline{\beta_{15}}(WAI)(Tmin) + \underline{\beta_{16}}(BA)(WAI) + \underline{\beta_{17}}(BA)(Tmin) + \underline{\beta_{18}}(BA)(TA) + \underline{\beta_{19}}(BA)(PA) +$

274    $\underline{\beta_{20}}(d_m)(WAI) + \underline{\beta_{21}}(d_m)(Tmin) + \underline{\beta_{22}}(d_m)(TA) + \underline{\beta_{23}}(d_m)(PA) + \underline{\beta_{24}}(WAI)(TA) +$

275    $\underline{\beta_{25}}(WAI)(PA) + (\underline{\beta_{26}}(Tmin)(TA)$ (1)

276

277   where the response variable is the absolute stand basal area change (SBAc), and the

278   numerical predictor variables were: stand basal area (BA), mean d.b.h. (d_m), minimum

279   temperatures (Tmin) and precipitation anomalies (PA) as quadratic terms; and water

280   availability (WAI) and temperature anomalies (TA) as linear terms (see Table 2 and

281   supplementary Table S4 for model comparisons, Table 3 for fitted parameter values,

282   supplementary Figure S4 for observed and predicted SBAc and supplementary Figure

283   S5 for model residuals). Country (i.e. Spain, Germany and Finland) was included as a

284   fixed categorical effect and thus linear terms were also included for Spain (SP) and

285   Finland (FI).

286   BIC model comparisons indicated that mean d.b.h. had the largest effect on

287   SBAc, followed by WAI, stand basal area, temperature anomaly and minimum

288   temperature (Table 2). The relative precipitation anomaly explained the smallest

289   variation compared to the rest of explanatory variables (Table 2). With regards to the

290   interaction terms, it is important to note that the full model included all possible pair-

291   wise interactions between the stand structure and climatic variables, but also strong

292   interactions between climate and recent climatic anomalies were found (Table 2,3).

293   The largest SBAc was observed in stands dominated by small trees (d_m< 200

294 mm). SBAc decreased rapidly with mean tree diameter up to *c.* ~~9~~800 mm after which it

295 increased again (Figure 2). Considering stand basal area, SBAc increased from low to

296 medium stand basal area values, stabilising from medium to high stand basal area

297 values (Figure 2).

298   The effect of WAI on SBAc was particularly strong in stands with low mean

299 d.b.h. (Figure 3a) and low basal area (Figure 3b). With increasing minimum

300 temperature, a non-linear relationship with SBAc was observed with a SBAc peak at

301 intermediate temperatures (Figure 4c), but this relationship was strongly affected by

302 mean d.b.h. (Figure 3c) and stand basal area (Figure 3d). The positive effect of

303 increasing minimum temperature on SBAc was particularly strong at high mean d.b.h.,

304 showing a more neutral relationship at low mean d.b.h. (Figure 3c). Stands with low

305 basal area showed the lowest SBAc at negative minimum temperatures, and the highest

306 SBAc at high basal area (Figure 3d). Moreover, we observed that the effect of minimum

307 temperature on SBAc was greater in wet areas (WAI positive) than in dry areas (WAI

308 negative) (Figure 4a). SBAc was positively associated with water availability (i.e. WAI)

309 in hot regions (i.e. Figure 4a,b) but no such relationship was found in regions with low

310 minimum temperatures (Figure 4a).

311   We observed an increase in SBAc with increases in recent temperature

312 anomalies (see positive value of parameter $\underline{\beta_9}$, Table 3). This positive effect of recent

313 warming on SBAc was particularly strong in stands with low mean d.b.h. (Figure 3e)

314 and high basal area (Figure 3f). The positive effect of recent temperature increase on

315 SBAc was also particularly high in wet areas, turning to neutral in dry sites (Figure 4b).

316 The positive effect of recent temperature increase was observed along the full length of

317 the minimum temperature gradient and was particularly strong at low minimum

318   temperatures (Figure 4c). The negative effects of recent precipitation reductions on

319   SBAc increments were observed in both dry and wet areas, but the positive effects of

320   precipitation increase only occurred in wet areas (i.e. positive WAI, Figure 4d).

321   **DISCUSSION**

322   The plot-based forest inventory information from Spain, Germany and Finland showed

323   that in the late 20th century undisturbed European forests experienced a net increase in

324   stand basal area, in agreement with previous studies (e.g. Ciais and others 2008;

325   Bellassen and others 2011). These increments were particularly large in the temperate

326   biome, turning to neutral or even negative in some areas of the Mediterranean and

327   northern boreal forests. Patterns of stand basal area increase were highly influenced by

328   stand structure (mean d.b.h. and stand basal area) and climate (water availability and

329   minimum temperatures), but also by recent temperature and precipitation anomalies.

330   The largest stand basal area changes (SBAc) occurred in relatively young forests or

331   forests in early development stages (i.e. low mean d.b.h. and low-medium basal area) in

332   mesic environments (i.e. not constrained by water or energy availability). Together,

333   these results suggest that the carbon sink potential of European forests could be strongly

334   constrained in water-limited Mediterranean forests, where the positive effects of recent

335   climate warming may be offset by competition and climatic stress.

336   **Patterns of stand basal area change and its components**

337   All three biomes showed a net increase in stand basal area, in agreement with previous

338   studies that have reported a general increase in biomass in the second half of the 20th

339   century (Kauppi and others 1992; Ciais and others 2008; Bellassen and others 2011; Pan

340   and others 2011). The positive correlation between stand basal area change (SBAc) and

341   growth suggests that factors controlling tree growth, such as stand structure, climate and

342   recent climatic anomalies are fundamental drivers of SBAc (Gómez-Aparicio and others

343   2011; Vayreda and others 2012). However, we observed a negative correlation between

344   SBAc and stand loss suggesting that stochastic mortality processes may have a key role

345   in the future on aboveground productivity and forest structure, particularly under

346   climate change (Allen and others 2010; Benito-Garzón and others 2013; Ruiz-Benito

347   and others 2013). These results suggest that both growth and mortality could potentially

348   affect species performance and future species distribution (Benito-Garzón and others

349   2013).

350   The temperate biome had the highest SBAc increments, which agrees with

351   global analyses of the aboveground forest carbon sink (Pan and others 2013). The

352   largest SBAc increments in temperate forest are probably due to increased tree growth

353   in parts of the latitudinal gradient not strongly limited by temperature or water

354   availability (e.g. Gerten and others 2008). It has been suggested that temperature

355   controls tree growth in boreal forests, whereas moisture and water availability are key

356   drivers in central and southern Europe (e.g. Vayreda and others 2012; Babst and others

357   2013). The highest mortality rates were observed in the Spanish part of the temperate

358   biome, probably due to the fact that the Iberian Peninsula harbours the southern

359   distribution limit of several widespread European species (Hewitt 2000; Hampe and

360   Petit 2005). In high-density Iberian forests increased temperature and drought events

361   have been related to tree mortality and forest decline (e.g. Carnicer and others 2011;

362   Sánchez-Salguero and others 2012; Ruiz-Benito and others 2013), most likely due to an

363   increase in tree density resulting from a reduction in management practices throughout

364   the Iberian Peninsula (e.g. Madrigal 1998; Ruiz-Benito and others 2012). Moreover,

365   most data from the Iberian Peninsula covers the early 21th century coinciding with the

366   severe drought of the 2000s (see Table S1), of which the effects on European forest

367   primary productivity have already been reported (Ciais and others 2005).

Structural and climatic factors determining stand basal area change

369   Mean d.b.h. was the variable with the highest overall effect on basal area change,

370   followed by water availability and stand basal area (Table 2). Mean d.b.h. and stand

371   basal area are both related to stand age, and reflect past disturbances (e.g. fire or logging

372   history). Our results are consistent with other studies that found that structural variables

373   are particularly important in driving biomass changes, and thus growth and mortality

374   processes (e.g. Vilá-Cabrera and others 2011; Vayreda and others 2012). Stand age has

375   been shown to be particularly important in the net ecosystem productivity of different

376   forest types including boreal and temperate broadleaved forests (Magnani and others

377   2007).

378   The high SBAc observed at medium stand basal area and low mean d.b.h. (see

379   Figure 2 and supplementary Figure S1 and S2) suggests that European forests could be

380   in competitive thinning stages and that they will continue to act as carbon sinks in the

381   near future (Ciais and others 2008; Vayreda and others 2012). The form of the

382   relationship between SBAc and stand basal area is similar to the well-known pattern for

383   above-ground biomass increment, which often increases with stand basal area then

384   levels off at higher population densities (e.g. Charru and others 2010; McMahon and

385   others 2010). Our results agree with typical forest development, where relatively young

386   stands accumulate carbon (i.e. in developing stages), but biomass increments start to

387   decline when the stands are at high competitive levels (i.e. intermediate mean d.b.h. and

388   high stand basal area, Coomes and Allen 2007).

389   Water availability had a strong, linear influence on SBAc (Table 2, Figure 3a,b),

390   emphasising the central role that heat and water stress have in driving growth and

391   mortality and, thus, are fundamental factors of carbon balance (Magnani and others

392   2007; Charruand others 2010). The positive effect of water availability on SBAc was

393   particularly pronounced in relatively young forest (i.e. low mean d.b.h. and low stand

394   basal area) and in hot areas (i.e. high minimum temperatures). Although differential

395   sensitivity in tree growth and tree mortality with age have been reported, greater

396   sensitivities have been found in either young trees (e.g. Suarez and others 2004; Vieira

397   and others 2009) or older trees (possibly related to hydraulic limitation, see Carrer and

398   Urbinati 2004). Our results suggest that relatively young forests or forests in developing

399   stages are particularly sensitive to low water availability and temperature-related stress

400   (see Coll and others 2013; Madrigal-González and Zavala 2014).

401   The relationship between SBAc and the minimum temperature gradient reflects

402   the large gradient covered from cold boreal to warm Mediterranean forests (see Figure

403   3c,d), which is a primary factor influencing tree species distributions (Woodward and

404   Williams 1987). Moreover, we observed that minimum temperatures had a positive

405   correlation with SBAc in forests with high mean d.b.h., low stand basal area or positive

406   water availability (Figure 3c,d and Figure 4a, respectively). This result suggests that

407   minimum temperature could be an important factor limiting primary productivity in

408   northern European forests (i.e. WAI positive and minimum temperature lower than -8

409   ºC, see supplementary Figure S1), but in southern dry forests water availability is the

410   main constraint (Boisvenue and Running 2006).

411   **Effect of recent temperature and precipitation anomalies on stand**

412   **basal area change**

413 Recent climate change has had a profound impact on SBAc. Increases in temperature

414 and precipitation were associated with increased SBAc (Figure 3e-g), and although its

415 effect was lower than those of stand structure or mean climate, we observed significant

416 interactive effects (Fig 3,4). Vayreda and others (2012) found that recent shifts in

417 climate had important effects on biomass growth in Spanish forests, and reported that

418 this effect had less influence on growth than stand structure or spatial climatic

419 variability. Sala and others (2012) have also suggested that productivity is more affected

420 by spatial than temporal variation in climate.

421 The general positive effect of increased temperature on basal area increments

422 observed in wet areas, agrees with other studies that have reported this effect when

423 water is not a limiting factor (McMahon and others 2010; Vayreda and others 2012).

424 Thus, warming could particularly enhance plant growth in boreal and temperate

425 European forests because of increases in metabolic rates (Anderson and others 2006;

426 Way and Oren, 2010) or longer growing seasons (Myneni and others 1991). In our

427 study, the trend for increased SBAc with increasing recent temperatures was observed

428 in relatively young forests, which are likely to be in a growth peak (Gómez-Aparicio

429 and others 2011). Overall, these results suggest that the positive effects of warming on

430 SBAc could vary greatly, depending on climate and stand structure. Thus stand basal

431 area increments could potentially be neutralised in water-limited forests, such as those

432 found in Mediterranean regions (see also Vayreda and others 2012), and in mature

433 forests where growth is generally less than forests in competitive thinning stages if there

434 is a slow filling of canopy gaps, or water or nutrient limitation (Coomes and others

435 2012).

436 Although the effect of recent shifts in precipitation on SBAc was much smaller

437 than the effect of increasing temperatures (Table 2), the relatively small SBAc in areas

438 with reduced precipitation was maintained along the entire water availability gradient

439 (Figure 4d), but was particularly important in wet areas (i.e. temperate and boreal

440 biomes). This result suggests that although drought stress could cause reduced growth

441 (Barber and others 2000; Silva and others 2010) rainfall shortage could also cause

442 important decreases in productivity (Ciais and others 2005). This could be particularly

443 severe in wet compared to dry areas, probably due to the poor adaptation of plants to

444 water shortages in these regions (Vicente-Serrano and others 2013). Nevertheless, in dry

445 sites, such as water-limited Mediterranean forests, temporal increases in precipitation

446 correlated with increases in SBAc (Figure 4d). This result suggests that water-limited

447 areas can be expected to respond to any increasing precipitation with large biomass

448 increments (e.g. Knapp and Smith 2001; Gerten and others 2008).

449 **Implications for stand basal area change in European forests**

450 This work provides support for the view that stand structure and climatic heterogeneity

451 are critical drivers of stand basal area change. These drivers should be taken into

452 account when determining the potential carbon sink or source of European forests over

453 time across biomes, because limiting factors and possible trends may radically differ

454 depending on climatic and structural conditions.

455 We observed a high net annual increment in recent stand basal area change of

456 0.43 m^2 ha^{-1} yr^{-1}, mainly due to stand basal area gains (*c.* 3.8%) and partially

457 constrained by stand basal area losses due to mortality (*c.* 0.06%, Table 1). A large

458 fraction of European forests are undergoing post-disturbance secondary succession

459 (including management practices)European forests are recovering from disturbances

460 and are undergoing management, which could be an explanation for the sink role

461 observed during the 1990s (e.g. Schimel and others 2001). Despite of the relatively high

increase in stand basal area in the period considered in this study, we observed a high
variability in the response. Our results suggest that the changes in basal area are highly
influenced by interactive effects between stand structure, climate and climate warming.
The repeated inventory-based measures used in this study highlight the potential role of
forests in accumulating biomass, but our results suggest that current stand structure (i.e.
the relatively young age and high density of European forests) and the potential effects
of spatial and temporal variations in climate could constrain biomass increases in the
absence of disturbances or other management actions (e.g. fire or extensive
management were not explicitly considered in this study). On the one hand, we
observed that relatively young forests or forests in competitive thinning stages have a
greater potential to act as aboveground carbon sinks than mature forest (e.g. Luyssaert
and others 2010; Pan and others 2011), however large areas of European forests are
increasing in density which may result in biomass increments levelling off (e.g. Charru
and others 2010). In addition, the largest increments in stand basal area were observed
in forests least limited by water or temperature, and the carbon sink role of European
forests could be strongly modulated by climate change. Stand basal area change could
be caused by either reduced forest growth or increased tree mortality, and thus may
affect species distributions (Benito-Garzón and others 2013). Moreover, rapid climate
warming may cause large-scale dieback in some forests (e.g. Allen and others 2010),
increased mortality or reduced growth caused by interactions between climate and stand
structure (e.g. Gómez-Aparicio and others 2011; Ruiz-Benito and others 2013).

Limitations in water and/or energy availability are fundamental drivers
constraining biomass increment (e.g. Boisvenue and Running 2006), as demonstrated by
the fact that Mediterranean (dry areas limited by water availability) and northern boreal
forests (limited by minimum temperature) had the lowest SBAc increments. Biomass

487 increments in Mediterranean water-limited forests have been relatively less affected by

488 recent climate warming compared to stands in temperate and boreal biomes (i.e. see

489 reduced SBAc response to increased temperature, Fig. 4b). However, basal area

490 accumulation due to the positive effects of climate warming is unlikely to continue at its

491 current rate in regions where precipitation is declining and forests are ageing. Early

492 signs of carbon sink saturation have been observed in European forests (Narbuurs and

493 others 2013), congruent with our results because aboveground biomass increments are

494 strongly dependent on current forest structure (see also Vayreda and others 2012).

495 However, our results may overestimate the rate of aboveground basal area accumulation

496 in European forests because we deliberately excluded harvested plots from our analyses,

497 in which stand basal area could have dropped substantially. Overall, we suggest that

498 forests in developing stages constitute an important short-term aboveground carbon

499 sink, but these forests could be particularly vulnerable to climate stress and competition,

500 especially in the water-limited Mediterranean region.

511   **REFERENCES**

512   Allen CD, Macalady AK, Chenchouni H, Bachelet D, McDowell N, Vennetier M,
513   Kitzberger T, Rigling A, Breshears DD, Hogg EH, Gonzalez P, Fensham R, Zhang
514   Z, Castro J, Demidova N, Lim J-H, Allard G, Running SW, Semerci A, Cobb N.
515   2010. A global overview of drought and heat-induced tree mortality reveals
516   emerging climate change risks for forests. Forest Ecology and Management 259:
517   660-684.

518   Anderson KJ, Allen AP, Gillooly JF, Brown JH. 2006. Temperature-dependence of
519   biomass accumulation rates during secondary succession. Ecology Letters 9: 673-
520   682.

521   Babst F, Poulter B, Trouet V, Tan K, Neuwirth B, Wilson R, Carrer M, Grabner M,
522   Tegel W, Levanic T, Panayotov M, Urbinati C, Bouriaud O, Ciais P, Frank
523   D.2013.Site- and species-specific responses of forest growth to climate across the
524   European continent. Global Ecology and Biogeography 22: 706-717.

525   Barber VA, Juday GP, Finney BP. 2000. Reduced growth of Alaskan white spruce
526   in the twentieth century from temperature-induced drought stress. Nature 405: 668-
527   673.

528   Bates D, Maechler M, Bolker B. 2012.lme4: Linear mixed-effects models using S4
529   classes. R-package version 0.999375-42.http://lme4.r-forge.r-project.org/.

530   Bellassen V, Luyssaert S (2014) Carbon sequestration: Managing forest in uncertain
531   times. Nature 506: 153-155.

532   Bellassen V, Viovy N, Luyssaert S, Le Maire G, Schelhaas MJ, Ciais P. 2011.
533   Reconstruction and attribution of the carbon sink of European forests between 1950
534   and 2000. Global Change Biology 17: 3274-3292.

535   Belsey DA. 1991. Conditioning diagnostics, collinearity and weak data in
536   regression. New York: Wiley.

537   Bolker BM, Brooks ME, Clark CJ, Geange SW, Poulsen JR, Stevens MHH, White
538   J-SS. 2009. Generalized linear mixed models: a practical guide for ecology and
539   evolution. Trends in Ecology & Evolution 24: 127-135.

540   Benito-Garzón M, Ruiz-Benito P, Zavala MA. 2013. Inter-specific differences in
541   tree growth and mortality responses to climate determine potential species
542   distribution limits in Iberian forests. Global Ecology and Biogeography 22: 1141-
543   1151.

544   Boisvenue C, Running SW. 2006. Impacts of climate change on natural forest
545   productivity – evidence since the middle of the 20th century. Global Change Biology
546   12: 862-882.

547 Burnham KP, Anderson DR. 2002. Model Selection and Multi model Inference: A
548 Practical Information-theoretic Approach. New York: Springer-Verlag New York.
549 488p.

550 Cao M, Woodward FI. 1998. Dynamic responses of terrestrial ecosystem carbon
551 cycling to global climate change. Nature 393: 249-252.

552 Canadell JG, Raupach MR. 2008. Managing forests for climate change mitigation.
553 Science 320: 1456-1457.

554 Carrer M, Urbinati C. 2004. Age-dependent tree-ring growth responses to climate in
555 *Larix decidua* and *Pinus cembra*. Ecology 85: 730-740.

556 Carnicer J, Coll M, Ninyerola M, Pons X, Sánchez G, Peñuelas J. 2011. Widespread
557 crown condition decline, food web disruption, and amplified tree mortality with
558 increased climate change-type drought. Proceedings of the National Academy of
559 Sciences 108: 1474-1478.

560 Charru M, SeynaveI, Morneau F, Bontemps JD. 2010. Recent changes in forest
561 productivity: An analysis of national forest inventory data for common beech
562 (*Fagus sylvatica* L.) in north-eastern France. Forest Ecology and Management 260:
563 864-874.

564 Christensen JH, Hewitson B, Busuioc A,Chen A, Gao X, Held I, Jones R, Kolli RK,
565 Kwon WT, Laprise R, Magaña Rueda V, Mearns L, Menéndez CG, Räisänen J,
566 Rinke A, Sarr A, Whetton P. 2007. Regional climate projections. Solomon S, Qin D,
567 Manning M, Chen Z, Marquis M, Averyt KB, Tignor M, Miller HL, editors.
568 Climate change 2007: The physical science basis. Cambridge: University Press.
569 p847-943.

570 Ciais P, Reichstein M, Viovy N, Granier A, Ogee J, Allard V, Aubinet M,
571 Buchmann N, Bernhofer C, Carrara A, Chevallier F, De Noblet N, Friend AD,
572 Friedlingstein P, Grunwald T, Heinesch B, Keronen P, Knohl A, Krinner G, Loustau
573 D, Manca G, Matteucci G, Miglietta F, Ourcival JM, Papale D, Pilegaard K, Rambal
574 S, Seufert G, Soussana JF, Sanz MJ, Schulze ED, Vesala T, Valentini R. 2005.
575 Europe-wide reduction in primary productivity caused by the heat and drought in
576 2003. Nature 437: 529-533.

577 Ciais P, Schelhaas MJ, Zaehle S,Piao SL, Cescatti A, Liski J, Luyssaert S, Le-Maire
578 G, Schulze E-D, Bouriaud O, Freibauer A, Valentini R, Nabuurs GJ. 2008. Carbon
579 accumulation in European forests. Nature Geosciences 1: 425-429.

580 Coll M, Peñuelas J, Ninyerola M, Pons X, Carnicer J. 2013. Multivariate effect
581 gradients driving forest demographic responses in the Iberian Peninsula. Forest
582 Ecology and Management 303: 195-209.

583   Coomes DA, Allen RB. 2007. Effects of size, competition and altitude on tree
584   growth. Journal of Ecology 95: 1084-1097.

585   Coomes DA, Holdaway RJ, Kobe RK, Lines ER, Allen RB. 2012. A general
586   integrative framework for modelling woody biomass production and carbon
587   sequestration rates in forests. Journal of Ecology 100: 42-64.

588   Dietze MC, Moorcroft PR. 2011. Tree mortality in the eastern and central United
589   States: patterns and drivers. Global Change Biology 17: 3312-3326.

590   Dixon RK, Solomon AM, Brown S, Houghton RA, Trexier MC, Wisniewski J.
591   1994. Carbon pools and flux of global forest ecosystems. Science 263: 185-190.

592   Food and Agriculture Organization of the United Nations. 2010. Global Forest
593   Resources Assessment 2010. http://www.fao.org/forestry/fra/fra2010/en/

594   Gamfeldt L, Snall T, Bagchi R,Jonsson M, Gustafsson L, Kjellander P, Ruiz-Jaen
595   MC, Froberg M, Stendahl J, Philipson CD, Mikusinski G, Andersson E, Westerlund
596   B, Andren H, Moberg F, Moen J, Bengtsson J. 2013. Higher levels of multiple
597   ecosystem services are found in forests with more tree species. Nature
598   Communications 4: 1340.

599   García-Valdés R, Zavala MA, Araújo MB, Purves DW. 2013. Chasing a moving
600   target: projecting climate change-induced changes in non-equilibrial tree species
601   distributions. Journal of Ecology 101: 441-453.

602   Gerten D, Luo Y, Le MaireG,Parton WJ, Keough C, Weng E, Beier C, Ciais P,
603   Cramer W, Dukes JS, Hanson PJ, Knapp AAK, Linder S, Nepstad DAN, Rustad L,
604   Sowerby A. 2008. Modelled effects of precipitation on ecosystem carbon and water
605   dynamics in different climatic zones. Global Change Biology 14: 2365-2379.

606   Gómez-Aparicio L, García-Valdés R, Ruiz-Benito P, Zavala MA. 2011.
607   Disentangling the relative importance of climate, size and competition on tree
608   growth in Iberian forests: implications for management under global change. Global
609   Change Biology 17: 2400-2414.

610   Goodale CL, Apps MJ, Birdsey RA, Field CB, Heath LS, Houghton RA, Jenkins
611   JC, Kohlmaier GH, Kurz W, Liu S, Nabuurs G-J, Nilsson S, Shvidenko AZ. 2002.
612   Forest carbon sinks in the northern hemisphere. Ecological Applications 12: 891-
613   899.

614   Hampe A, Petit RJ. 2005. Conserving biodiversity under climate change: the rear
615   edge matters. Ecology Letters 8: 461-467.

616   Hember RA, Kurz WA, Metsaranta JM, Black TA, Guy RD, Coops NC. 2012.
617   Accelerating regrowth of temperate-maritime forests due to environmental change.
618   Global Change Biology 18: 2026-2040.

619   Hewitt G. 2000. The genetic legacy of the Quaternary ice ages. Nature 405: 907-
620   913.

621   Hijmans RJ, Cameron SE, Parra JL, Jones PG, Jarvis A. 2005.Very high resolution
622   interpolated climate surfaces for global land areas. International Journal of
623   Climatology 25: 1965-1978.

624   Hilborn R, Mangel M. 1997. The ecological detective: confronting models with
625   data. Princeton (NJ): Princeton University Press.

626   Hoch G, Körner C. 2012. Global patterns of mobile carbon stores in trees at the
627   high-elevation tree line. Global Ecology and Biogeography 21: 861-871.

628   Lines ER, Zavala MA, Purves DW, Coomes DA. 2012. Predictable changes in
629   aboveground allometry of trees along gradients of temperature, aridity and
630   competition. Global Ecology and Biogeography 21: 1017-1028.

631   Kauppi PE, Mielikäinen K, Kuusela K. 1992. Biomass and carbon budget of
632   European forests, 1971 to 1990. Science 256: 70-74.

633   Knapp AK, Smith MD. 2001. Variation among biomes in temporal dynamics of
634   aboveground primary production. Science 291: 481-484.

635   Kunstler G, Albert CH, Courbaud B, Lavergne S, Thuiller W, Vieilledent G,
636   Zimmermann NE, Coomes DA. 2011. Effects of competition on tree radial-growth
637   vary in importance but not in intensity along climatic gradients. Journal of Ecology
638   99: 300-312.

639   Luo Y, Gerten D, Le Maire G,Parton WJ, Weng E, Zhou X, Keough C, Beier C,
640   Ciais P, Cramer W, Dukes JS, Emmett B, Hanson PJ, Knapp A, Linder S, Nepstad
641   DAN, Rustad L. 2008. Modeled interactive effects of precipitation, temperature, and
642   [CO_2] on ecosystem carbon and water dynamics in different climatic zones. Global
643   Change Biology 14: 1986-1999.

644   Luyssaert S, Ciais P, Piao SL, Schulze ED, Jung M, Zaehle S, Schelhaas MJ,
645   Reichstein M, Churkina G, Papale D, Abril G, Beer C, Grace J, Loustau D,
646   Matteucci G, Magnani F, Nabuurs GJ, Verbeeck H, Sulkava M, Van Der Werf GR,
647   Janssens IA. 2010. The European carbon balance. Part 3: Forests. Global Change
648   Biology 16: 1429-1450.

649   Madrigal A. 1998. Problemática de la ordenación de masas artificiales en España.
650   Cuadernos de la Sociedad Española de Ciencias Forestales 6: 13-20.

651   Magnani F, Mencuccini M, Borghetti M , Berbigier P, Berninger F, Delzon S,
652   Grelle A, Hari P, Jarvis PG, Kolari P, Kowalski AS, Lankreijer H, Law BE,
653   Lindroth A, Loustau D, Manca G, Moncrieff JB, Rayment M, Tedeschi V, Valentini

654 R, Grace J. 2007. The human footprint in the carbon cycle of temperate and boreal
655 forests. Nature 447: 849-851.

656 Madrigal-González J, Zavala MA. 2014. Competition and tree age modulated last
657 century pine growth responses to high frequency of dry years in a water limited
658 forest ecosystem. Agricultural and Forest Meteorology 192-193: 18-26.

659 McMahon SM, Parker GG, Miller DR. 2010. Evidence for a recent increase in forest
660 growth. Proceedings of the National Academy of Sciences 107: 3611-3615.

661 Millennium Ecosystem Assessment. 2005. Ecosystem and human well-being:
662 biodiversity synthesis. Washington, DC: Island Press.

663 Myneni RB, Keeling CD, Tucker CJ, Asrar G, Nemani RR. 1991. Increased plant
664 growth in the northern high latitudes from 1981 to 1991. Nature 386: 698-702.

665 Nabuurs GJ, Lindner M, Verkerk PJ, Gunia K, Deda P, Michalak R, Grassi G. 2013.
666 First signs of carbon sink saturation in European forest biomass. Nature Climate
667 Change 3: 792-796.

668 Nabuurs GJ, Schelhaas MJ, Mohren GMJ, Field CB. 2003. Temporal evolution of
669 the European forest sector carbon sink from 1950 to 1999. Global Change Biology
670 9: 152-160.

671 Nakagawa S, Schielzeth H. 2013. A general and simple method for obtaining R^2
672 from generalized linear mixed-effects models. Methods in Ecology and Evolution 4:
673 133-142.

674 Oksanen J, Blanchet FG, Kindt R;Legendre P, O'Hara RG, Simpson GL, Solymos P,
675 Stevens M, Wagner H. 2010. Multivariate analysis of ecological communities in R:
676 vegan tutorial. R package version 1.17-0. http://CRAN.R-
677 project.org/package=vegan.

678 Olson DM, Dinerstein E, Wikramanayake ED, Burgess ND, Powell GVN,
679 Underwood EC, D'amico JA, Itoua I, Strand HE, Morrison JC, Loucks CJ, Allnutt
680 TF, Ricketts TH, Kura Y, Lamoreux JF, Wettengel WW, Hedao P, Kassem KR.
681 2001. Terrestrial ecoregions of the world: a new map of life on earth. Bioscience 51:
682 933-938.

683 Pan Y, Birdsey RA, Fang J,Houghton R, Kauppi PE, Kurz WA, Phillips OL,
684 Shvidenko A, Lewis SL, Canadell JG, Ciais P, Jackson RB, Pacala SW, McGuire
685 AD, Piao S, Rautiainen A, Sitch S, Hayes D. 2011. A large and persistent carbon
686 sink in the world's forests. Science 333: 988-993.

687 Pastor J, Post WM (1988) Response of northern forests to CO_2-induced climate
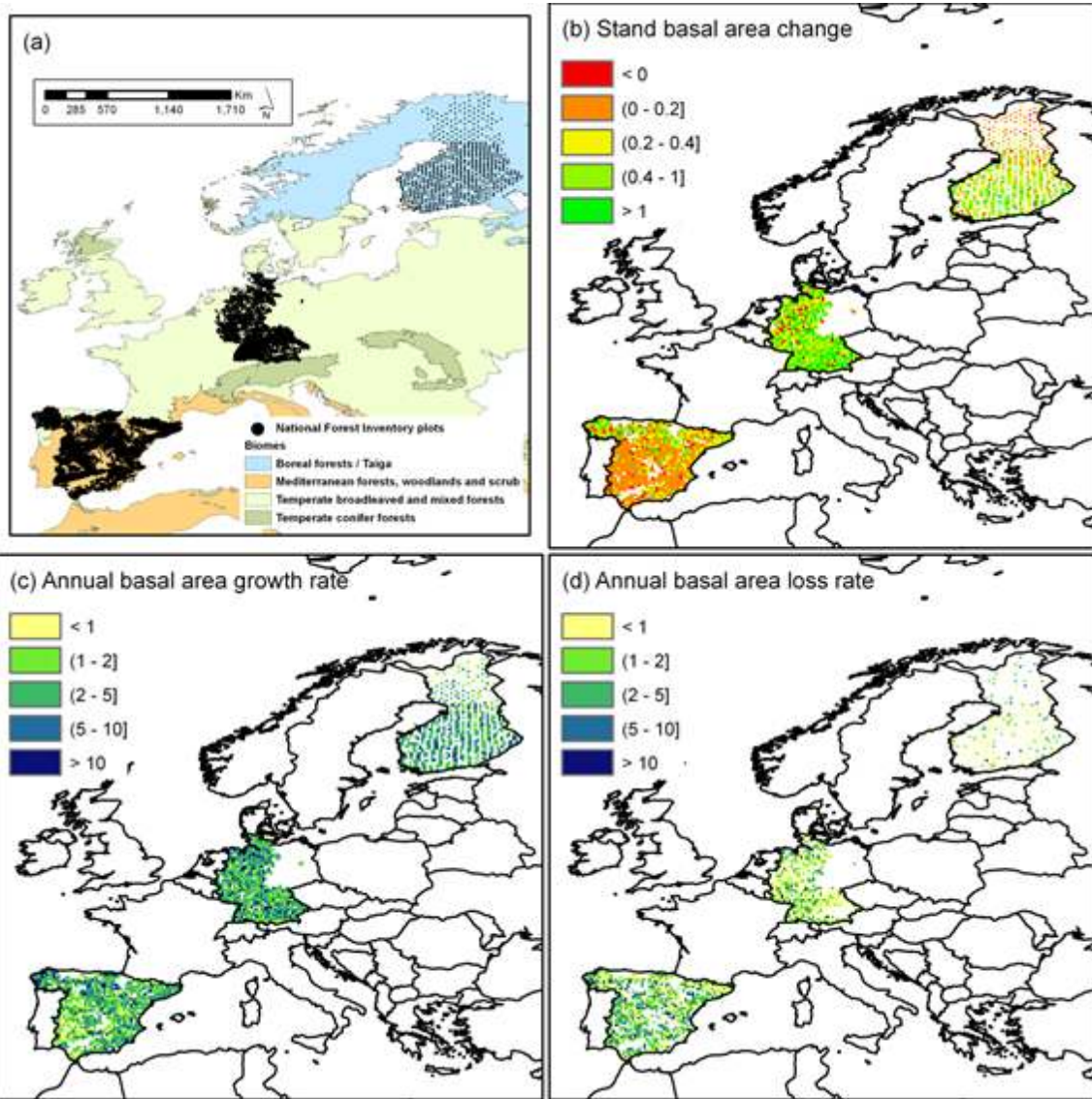688 change. Nature 334: 55-58.

689 Peng J, Dan L, Huang M. 2014. Sensitivity of global and regional terrestrial carbon
690 storage to the direct CO_2 effect and climate change based on the CMIP5 model
691 intercomparison. PLoS ONE 9: e95282.

692 Pinheiro JC, Bates DM. 2000. Mixed effect models in S and S-Plus. New York:
693 Springer-Verlag New York.528 p.

694 R Development Core Team. 2012. R: a language and environment for statistical
695 computing. Vienna: R Foundation for Statistical Computing. www.r-project.org.

696 Ruiz-Benito P, Gómez-Aparicio L, Zavala MA. 2012. Large scale assessment of
697 regeneration and diversity in Mediterranean planted pine forests along ecological
698 gradients. Diversity and Distributions 18: 1092–1106.

699 Ruiz-Benito P, Lines ER, Gómez-Aparicio L, Zavala MA, Coomes DA. 2013.
700 Patterns and drivers of tree mortality in Iberian forests: climatic effects are modified
701 by competition. PLoS ONE 8: e56843.

702 Sala OE, Gherardi LA, Reichmann L, Jobbágy E, Peters D. 2012. Legacies of
703 precipitation fluctuations on primary production: theory and data synthesis.
704 Philosophical Transactions of the Royal Society B: Biological Sciences 367: 3135-
705 3144.

706 Sánchez-Salguero R, Navarro-Cerrillo R, Camarero J, Fernández-Cancio Á. 2012.
707 Selective drought-induced decline of pine species in southeastern Spain. Climatic
708 Change 113: 767-785.

709 Schimel D. 2007. Carbon cycle conundrums. Proceedings of the National Academy
710 of Sciences 104: 18353-18354.

711 Schimel DS, House JI, Hibbard KA, Bousquet P, Ciais P, Peylin P, Braswell BH,
712 Apps MJ, Baker D, Bondeau A, Canadell J, Churkina G, Cramer W, Denning AS,
713 Field CB, Friedlingstein P, Goodale C, Heimann M, Houghton RA, Melillo JM,
714 Moore B, Murdiyarso D, Noble I, Pacala SW, Prentice IC, Raupach MR, Rayner PJ,
715 Scholes RJ, Steffen WL, Wirth C. 2001. Recent patterns and mechanisms of carbon
716 exchange by terrestrial ecosystems. Nature 414: 169-172.

717 Sheil D, Burslem DFRP, Alder D. 1995. The interpretation and misinterpretation of
718 mortality rate measures. Journal of Ecology 83: 331-333.

719 Slik JWF, Aiba S-I, Brearley FQ, Cannon CH, Forshed O, Kitayama K, Nagamasu
720 H, Nilus R, Payne J, Paoli G, Poulsen AD, Raes N, Sheil D, Sidiyasa K, Suzuki E,
721 van Valkenburg JLCH. 2010. Environmental correlates of tree biomass, basal area,
722 wood specific gravity and stem density gradients in Borneo's tropical forests. Global
723 Ecology and Biogeography 19: 50-60.

724   Silva LCR, Anand M, Leithead MD. 2010. Recent widespread tree growth decline
725   despite increasing atmospheric CO_2. PLoS ONE 5: e11543.

726   Suarez ML, Ghermandi L, Kitzberger T. 2004. Factors predisposing episodic
727   drought-induced tree mortality in *Nothofagus*– site, climatic sensitivity and growth
728   trends. Journal of Ecology 92: 954-966.

729   Spiecker H. 1999. Overview of recent growth trends in European forests. Water,
730   Air, & Soil Pollution 116: 33-46.

731   Sykes M, Prentice IC. 1996. Climate change, tree species distributions and forest
732   dynamics: A case study in the mixed conifer/northern hardwoods zone of Northern
733   Europe. Climatic Change 34: 161-177.

734   Valentini R, Matteucci G, Dolman AJ, Schulze E-D, Rebmann C, Moors EJ,
735   Granier A, Gross P, Jensen NO, Pilegaard K, Lindroth A, Grelle A, Bernhofer C,
736   Grunwald T, Aubinet M, Ceulemans R, Kowalski AS, Vesala T, Rannik U,
737   Berbigier P, Loustau D, Gu[eth]mundsson J, Thorgeirsson H, Ibrom A, Morgenstern
738   K, Clement R, Moncrieff J, Montagnani L, Minerbi S, Jarvis PG. 2000. Respiration
739   as the main determinant of carbon balance in European forests. Nature 404: 861-
740   865.

741   vanMantgem PJ, Stephenson NL, Byrne JC, Daniels LD, Franklin JF, Fule PZ,
742   Harmon ME, Larson AJ, Smith JM, Taylor AH, Veblen TT.2009. Widespread
743   increase of tree mortality rates in the western United States. Science 323: 521-524.

744   Vayreda J, Martínez-Vilalta J, Gracia M, Retana J. 2012. Recent climate changes
745   interact with stand structure and management to determine changes in tree carbon
746   stocks in Spanish forests. Global Change Biology 18: 1028-1041.

747   Vicente-Serrano SM, Gouveia C, Camarero, Beguería S, Trigo R, López-Moreno JI,
748   Azorín-Molina Cs, Pasho E, Lorenzo-Lacruz J, Revuelto J, Morán-Tejeda E,
749   Sánchez-Lorenzo A. 2013.Response of vegetation to drought time-scales across
750   global land biomes. Proceedings of the National Academy of Sciences 110: 52-57.

751   Vieira J, Campelo F, Nabais C. 2009. Age-dependent responses of tree-ring growth
752   and intra-annual density fluctuations of *Pinus pinaster* to Mediterranean climate.
753   Trees-Structure and Function 23: 257-265.

754   Vilá-Cabrera A, Martínez-Vilalta J, Vayreda J, Retana J. 2011. Structural and
755   climatic determinants of demographic rates of Scots pine forests across the Iberian
756   Peninsula. Ecological Applications 31: 1162-1172.

757   Vilà M, Carrillo-Gavilán A, Vayreda J, Bugmann H, Fridman J, Grodzki W, Haase
758   J, Kunstler G, Schelhaas M, Trasobares A. 2013 Disentangling biodiversity and
759   climatic determinants of wood production. PLoS ONE 8: e53530.

760 Way DA, Oren R. 2010. Differential responses to changes in growth temperature
761 between trees from different functional groups and biomes: a review and synthesis
762 of data. Tree Physiology 30: 669-688.

763 Woodward FI, Williams BG. 1987.Climate and plant distribution at global and local
764 scales.Vegetatio69: 189-197.

765 Zhao M, Running SW. 2010. Drought-induced reduction in global terrestrial net
766 primary production from 2000 through 2009. Science 329: 940-943.

767 Zomer R, Bossio D, Trabucco A, Yuanjie L, Gupta D, Singh V. 2007. Trees and
768 water: smallholder agroforestry on irrigated lands in Northern India. Colombo:
769 International Water Management Institute.

770 Zomer RJ, Trabucco A, Bossio DA, Verchot LV. 2008. Climate change mitigation:
771 A spatial analysis of global land suitability for clean development mechanism
772 afforestation and reforestation. Agriculture, Ecosystems & Environment 126: 67-80.

773 Zuur AF, Ieno EN, Walker NJ, Saveliev AA, Smith GM. 2009. Mixed effects
774 models and extension in ecology with R. New York: Springer.

775
776 **Figure 1.**

777

778   **Figure 2.**

Ruiz-Benito *et al.* 33

779
780   **Figure 3.**

781

782 **Figure 4.**

783   **FIGURE LEGENDS**

784   **Figure 1.** Map of Spanish, German and Finnish NFI at a spatial resolution of 0.2 x 0.2

785   degrees: (a) the stands included in this study and the underlying biome distribution

786   (Olson and others 2001), and the spatial distribution of (b) stand basal area change

787   (SBAc, m^2 ha^{-1} yr^{-1}), (c) annual basal area growth rate (SBA$_{gain}$, % yr^{-1}), (d) annual loss

788   rate (SBA$_{loss}$, % yr^{-1}).

789   **Figure 2.** Predicted basal area change (m^2 ha^{-1} yr^{-1}) by mean d.b.h. (mm) and stand

790   basal area (m^2 ha^{-1}).

791   **Figure 3.** Predicted basal area change in relation to climatic variables in two

792   combinations of mean d.b.h. and basal area. The predicted variation in basal area

793   change (m^2 ha^{-1} yr^{-1}, i.e. proxy of biomass change) and 95% confidence intervals were

794   calculated for two combinations of mean d.b.h. (99 percentiles showing high and low

795   d.b.h.) and stand basal area (99 percentiles showing high and low basal area) along:

796   (a,b) water availability (%), (c,d) minimum temperatures, (e,f) temperature anomaly,

797   and (g) precipitation anomaly. The effect of precipitation anomaly on stand basal area

798   change is only shown for combinations of stand basal area, because the interaction

799   between precipitation anomaly and mean d.b.h. did not support a substantial

800   improvement in the model (see Table 2).

801   **Figure 4.** Predicted basal area change against main interactions between climatic

802   variables. Tridimensional plot showing the predicted effects on basal area change (m^2

803   ha^{-1} yr^{-1}) of the main interactions: (a) water availability $\times$ minimum temperature, (b)

804   water availability $\times$ temperature anomaly, (c) minimum temperature $\times$ temperature

805   anomaly, and (d) water availability $\times$ precipitation anomaly.

806   **Table 1.** Summary statistics of the inventory plots.

	Mediterranean	**Temperate**	**Boreal**	**All data**
SBAc (m^2 ha^{-1} yr^{-1})	0.28 ± 0.003 [-0.25, 1.39]	0.71 ± 0.006 [-0.41, 2.43]	0.47 ± 0.009 [-0.05, 1.31]	0.43 ± 0.003 [-0.29, 1.98]
SBA_{gain} (% yr^{-1})	3.36 ± 0.046 [0.36, 12.94]	4.59 ± 0.046 [0.71, 20.13]	4.34 ± 4.524 [0.36, 14.00]	3.82 ± 0.021 [0.44, 15.55]
SBA_{loss} (% yr^{-1})	0.61 ± 0.013 [0.00, 6.47]	0.63 ± 0.017 [0.00, 5.53]	0.21 ± 0.021 [0.00, 2.06]	0.6 ± 0.000 [0.00, 6.06]
BA (m^2 ha^{-1})	8.82 ± 0.06 [0.60, 33.43]	21.77 ± 0.12 [1.75, 55.52]	10.1 ± 0.21 [0.34, 29.91]	13.34 ± 0.06 [0.67, 46.17]
d_m (mm)	261.49 ± 0.86 [115.00, 612.60]	284.13 ± 1.06 [113.47, 572.81]	165.25 ± 1.2 [106.83, 284.54]	265.4 ± 0.66 [113.00, 591.92]
WAI (%)	-42.46 ± 0.12 [-67.55, 6.15]	19.77 ± 0.25 [-17.82, 94.48]	15.77 ± 0.21 [0.55, 30.36]	-18.67 ± 0.19 [-65.86, 63.99]
Tmin (ºC)	5.45 ± 0.17 [0.90, 10.60]	1.3 ± 0.24 [-3.00, 8.40]	-9.62 ± 0.56 [-14.60, -5.60]	3.42 ± 0.21 [-8.70, 10.10]
TA (ºC)	0.57 ± 0 [0.30 ,0.90]	0.32 ± 0 [0.00 ,0.70]	0.1 ± 0 [0.00 ,0.30]	0.46 ± 0 [0.00 ,0.90]
PA (%)	-3.44 ± 0.02 [-9.38, 2.04]	-1.74 ± 0.03 [-7.69, 3.70]	3.73 ± 0.07 [-2.00, 8.89]	-2.56 ± 0.02 [-8.33, 4.08]
No. Plots (%)	61.52%	34.48%	4.00%	100.00%

807　**Table 2.** Alternative models of stand basal area change.

(a) Main and interaction effect models	BIC	ΔBIC	(b) Main effect models	BIC	ΔBIC
Full	**57946**	**0**	**Full**	**58934**	**0**
No Precipitation anomaly	57959	13	No Precipitation anomaly	58937	3
No Min. temperature	58136	190	No Min. temperature	59018	84
No Temperature anomaly	58229	283	No Temperature anomaly	59085	151
No Stand basal area	58552	606	No Stand basal area	59506	572
No Water availability	59358	1412	No Water availability	60230	1296
No Mean d.b.h.	61285	3339	No Mean d.b.h.	62296	3362

(c) Interaction effect models

	BIC	ΔBIC
Full	**57946**	**0**
No (Mean d.b.h. × Precipitation anomaly)	57949	3
No (Stand basal area × Mean d.b.h.)	57950	4
No (Mean d.b.h. × Temperature anomaly)	57955	9
No (Stand basal area × Precipitation anomaly)	57963	17
No (Min. temperature × Temperature anomaly)	57964	18
No (Stand basal area × Min. temperature)	57971	25
No (Water availability × Temperature anomaly)	57974	28
No (Stand basal area × Water availability)	57983	37
No (Water availability × Precipitation anomaly)	57984	38
No (Mean d.b.h. × Min. temperature)	57993	47
No (Stand basal area × Temperature anomaly)	58044	98
No (Water availability × Min. temperature)	58053	107
No (Mean d.b.h. × Water availability)	58071	125

808

809

810   **Table 3.** Parameters of the final model of stand basal area change.

	Parameter	Mean	SE	LCI	UCI
Intercept	β_1	0.9142	0.0102	0.8960	0.9370
BA	β_2	0.0424	0.0042	0.0348	0.0498
BA^2	β_3	-0.0265	0.0020	-0.0302	-0.0229
d_m	β_4	-0.1983	0.0035	-0.2055	-0.1911
$d_m{}^2$	β_5	0.0327	0.0013	0.0296	0.0356
WAI	β_6	0.1371	0.0037	0.1300	0.1442
Tmin	β_7	0.0161	0.0054	0.0064	0.0288
$Tmin^2$	β_8	-0.0115	0.0035	-0.0183	-0.0043
TA	β_9	0.0505	0.0040	0.0419	0.0603
PA	β_{10}	-0.0090	0.0034	-0.0156	-0.002
PA^2	β_{11}	-0.0075	0.0014	-0.0106	-0.0047
SP	β_{12}	-0.5614	0.0122	-0.5895	-0.5396
FI	β_{13}	-0.5288	0.0371	-0.5965	-0.447
BA × d_m	β_{14}	0.0065	0.0029	0.0009	0.0123
WAI × Tmin	β_{15}	0.0435	0.0042	0.0368	0.0517
BA × WAI	β_{16}	-0.0209	0.0034	-0.0279	-0.0131
BA × Tmin	β_{17}	-0.0215	0.0043	-0.0287	-0.0137
BA × TA	β_{18}	0.0336	0.0034	0.0273	0.0409
BA × PA	β_{19}	-0.0130	0.0031	-0.0185	-0.0063
d_m × WAI	β_{20}	-0.0431	0.0039	-0.0506	-0.0366
d_m × Tmin	β_{21}	0.0277	0.0040	0.0195	0.0349
d_m × TA	β_{22}	-0.0107	0.0036	-0.0182	-0.0038
d_m × PA	β_{23}	-0.0031	0.0027	-0.0096	0.0021
WAI × TA	β_{24}	0.0263	0.0050	0.0143	0.0366
WAI × PA	β_{25}	0.0249	0.0040	0.0168	0.0319
Tmin× TA	β_{26}	0.0215	0.0049	0.0112	0.0309

811

812   **TABLES LEGENDS**

813   **Table 1.** Summary statistics of the inventory plots.

814   Mean, standard error and 95% percentiles [min., max.] of stand basal area change

815   (SBAc, m^2 ha^{-1} yr^{-1}), basal area growth rate (SBA$_{gain}$, % yr^{-1}), basal area loss rate

816   (SBA$_{loss}$, % yr^{-1}), stand basal area (BA, m^2 ha^{-1}), mean d.b.h. (d$_m$, mm), water

817   availability (WAI, %), minimum temperature (Tmin, ºC), temperature anomaly (TA, ºC)

818   and precipitation anomaly (PA, %). Percentage of plots in boreal, temperate,

819   Mediterranean biomes is also shown.

820   **Table 2.** Alternative models of stand basal area change.

821   Comparisons of alternate models of stand basal area change (m^2 ha^{-1} yr^{-1}) based on

822   Bayesian Information Criterion (BIC): (a) to test main effects including pair-wise

823   interactions between explanatory variables (Main and interaction effect models, i.e.

824   ignore the effect of each predictor variable and the interactions where the variable is

825   involved), (b) to test main effects without include pair-wise interactions between

826   explanatory variables (Main effect models, i.e. ignore the effect of each predictor

827   variable without considering any interaction), and (c) to test only the individual effect of

828   the interactions (Interactions effect models). The full models include the effects of

829   mean d.b.h., stand basal area, minimum temperature, temperature anomaly, and

830   precipitation anomaly. The best fitting model is given in ΔBIC value of zero (bold),

831   comparing the full model with models dropping the effect of the predictor variables

832   considering the main effects and/or the interactions. Thus, the alternate models ignore

833   the effects ('No') of: (a) main effects of the predictor variables and the interactions

834   where the variable is involved, (b) main effects of the predictor variables without

835   interactions or (c) interactions.

836   **Table 3.** Parameters of the final model of stand basal area change.

837   Mean estimated parameters (Parameter), standard error (SE) and lower and upper 95%

838   confidence intervals (LCI and UCI, respectively) of the final model of basal area change

839   (see Eq. (1)).

1
2
3
4
5
6
7
8
9
10
11
12
13
14
15
16
17
18
19
20
21
22
23
24
25
26
27
28
29
30
31
32
33
34
35
36
37
38
39
40
41
42
43
44
45
46
47
48
49
50
51
52
53
54
55
56
57
58
59
60

Ruiz-Benito P, Madrigal-González J, Ratcliffe S, Coomes DA, Kändler G, Lehtonen A, Wirth C, Zavala MA. *Stand structure and recent climate change constrain stand basal area change in European forests: a comparison across boreal, temperate and Mediterranean biomes*

ELECTRONIC SUPPLEMENTARY MATERIAL

APPENDIX 1. DESCRIPTION OF NATIONAL FOREST INVENTORIES OF SPAIN, GERMANY AND

FINLAND

SPANISH NATIONAL FOREST INVENTORY

We used information from the second and third Spanish NFI (surveyed in the periods

1986-1996 and 1997-2007, respectively). The Spanish NFI plots are located on a 1 km^2

grid aver forested regions (Villaescusa and Díaz 1998; Villanueva 2004). The time

interval between surveys ranged from 6 to 13 years (mean 11.1 ± 0.9 years). Spanish

NFI plots were sampled using a v

ariable radius technique with four concentric circular subplots of radius 5, 10, 15 and 25

m. Within each subplot, trees were included in the sample according to their diameter at

breast height (d.b.h.), with trees of 7.5-12.4 cm measured in the 5 m radius subplot,

those of 12.5-22.4 cm in the 10 m radius subplot, those of 22.5-42.4 cm in the 15 m

radius subplot, and those with d.b.h. larger or equal to 42.5 cm in the 25 m radius

subplot.

GERMAN NATIONAL FOREST INVENTORY

We used information from the first and second German NFI. The German NFI uses a

systematic grid of clusters, sampled in the periods 1986-1990 and 2001-2002

respectively. The size of the sample grid is 4 by 4 km, however, it is reduced in some

federal states to either 2.83 by 2.83 km or 2 by 2 km. Each cluster is a quadrangle of

150 m in length with a sample plot on each corner. Trees with a d.b.h. of 10 cm or more

in the first inventory and 7 cm in the second were selected by the angle-count method

with a basal area factor (BAF) of 4 (m^2 ha^{-1}) if they are alive or recently dead.

FINNISH NATIONAL FOREST INVENTORY

We used data from the permanent sample plots of the Finnish NFI from two consecutive

surveys sampled in the periods 1985-1986 and 1995 (subset NFI8). This permanent

sample plot data has a systematic grid of plot clusters in forested areas (Mäkipää and

Heikkinen 2003). In Southern Finland the grid is 16 by 16 square km, with four plots in

each cluster at 400 m. intervals, while in Northern Finland the grid is a 24 by 32 km

rectangle with three plots per cluster, at 600 m. intervals. These permanent sample plot

data were sampled using a variable radius technique with two concentric circular

subplots of radius 5.64 m for trees under 10.5 cm d.b.h. and 9.77 m for trees of d.b.h.

10.5 cm or higher.

REFERENCES

Mäkipää R, Heikkinen J. 2003. Large-scale changes in abundance of terricolous
    bryophytes and macrolichens in Finland. Journal of Vegetation Science 14: 497–508.

Villaescusa R, Díaz R, Ed. 1998. Segundo Inventario Forestal Nacional (1986-1996).
    Madrid: Ed. Ministerio de Medio Ambiente, ICONA.

Villanueva JA, Ed. 2004. Tercer Inventario Forestal Nacional (1997-2007). Comunidad
    de Madrid. Madrid: Ed. Ministerio de Medio Ambiente.

APPENDIX 2. FURTHER DETAILS REGARDING SELECTION OF CLIMATIC VARIABLES.

Each of the NFI plots was characterized by 22 climatic variables from WorldClim (Hijmans and others 2005) and CGIAR-CSI GeoPortal, using CGIAR-CSI Global-Aridity and Global-PET Database (Zomer and others 2007; 2008). The relationship between the initial set of highly correlated climatic variables (see Table S2) was explored using Principal Component Analysis in R (R Development Core Team, 2012). The first axis of the PCA (explaining 54% of the variance) was strongly and positively correlated with potential water availability and negatively correlated with potential evapotranspiration. The second axis (explaining 24% of the variance) was strongly correlated with mean temperature of the coldest quarter (ºC) and temperature seasonality (ºC). To select which indicator of climate performed better we compared single-predictor models using quadratic functional forms which individually used water availability, potential evapotranspiration, minimum temperature and temperature seasonality as predictors of stand basal area change. The best predictors of climate (according to Bayesian Information Criteria, BIC) were water availability and minimum temperatures and were retained for our modeling analysis (Table S2.1).

Table S2.1. Comparison of stand basal area change models based on BIC parameterized variables that could be used as representative of climate. Predictor variables are WAI (water availability), PET (potential evapotranspiration), Tmin (minimum temperatures) and TS (Temperature seasonality). Number of parameter (NP), Bayesian Information Criterion (BIC) and ΔBIC are also shown.

Predictor	NP	BIC	ΔBIC
WAI	**3**	**66873**	**0**
PET	3	67365	492
Predictor	**NP**	**BIC**	**ΔBIC**
Tmin	**3**	**69166**	**0**
TS	3	72339	3172

REFERENCES

Hijmans RJ, Cameron SE, Parra JL, Jones PG, Jarvis A. 2005.Very high resolution interpolated climate surfaces for global land areas. International Journal of Climatology 25: 1965-1978.

R Development Core Team. 2012. R: a language and environment for statistical computing. Vienna: R Foundation for Statistical Computing. www.r-project.org.

Zomer R, Bossio D, Trabucco A, Yuanjie L, Gupta D, Singh V. 2007. Trees and water: smallholder agroforestry on irrigated lands in Northern India. Colombo: International Water Management Institute.

Zomer RJ, Trabucco A, Bossio DA, Verchot LV. 2008. Climate change mitigation: A spatial analysis of global land suitability for clean development mechanism afforestation and reforestation. Agriculture, Ecosystems & Environment 126: 67-80.

TABLE S1. Main characteristics of the plot and sampling design from the three National

Forest Inventories used in this study (see more details in Appendix S1).

	Finland	Germany	Spain
Survey dates	1985/86 - 1995	1986/90 - 2001/02	1986/96 - 1997/2007
Sample plot design	Cluster design, number and grid size depend on location. Mostly 6 x 6 km and 7 x 7 km grid. 250 or 300 m between plots in a cluster. 10, 11 or 14 plots in a cluster	Cluster design, 4 subplots. Grid size depends on region. Standard grid size is 4 by 4 km	1 by 1 km grid of single sample plots
Sample tree survey design	Variable radius	Angle-count	Variable radius
Plot size (m^2)	100, 300	Variable, Basal Area Factor (BAF) 4 m^2 ha^{-1}	79, 315, 707, 1964
Minimum tree d.b.h. (cm)	1	10, 7	7.5
No. plots included in study (percentage)	(4.00%)	(34.48%)	(61.52%)

1
2
3
4
5
6
7
8
9
10
11
12
13
14
15
16
17
18
19
20
21
22
23
24
25
26
27
28
29
30
31
32
33
34
35
36
37
38
39
40
41
42
43
44
45
46
47

TABLE S2. List of initial set of 22 climatic predictors of stand basal area change available from WorldClim (Hijmansand others 2005) and CGIAR-CSI GeoPortal, using CGIAR-CSI Global-Aridity and Global-PET Database (Zomer and others 2007; 2008).

CODE	VARIABLE	UNITS	DEFINITION
BIO1	Annual mean temperature	℃	The mean of all the weekly mean temperatures
BIO2	Mean diurnal range	℃	The mean of all the weekly diurnal temperature ranges
BIO3	Isothermality	%	The mean diurnal range divided by the annual temperature range
BIO4	Temperature seasonality	℃	Standard deviation *100
BIO5	Max temperature of warmest month	℃	Highest temperature of any weekly maximum temperature.
BIO6	Min temperature of coldest month	℃	Lowest temperature of any weekly minimum temperature.
BIO7	Temperature annual range	℃	Difference between BIO5 and BIO6

CODE	VARIABLE	UNITS	DEFINITION
BIO8	Mean temperature of wettest quarter	°C	The wettest quarter of the year is determined (to the nearest week), and the mean temperature of this period is calculated.
BIO9	Mean temperature of driest quarter	°C	The driest quarter of the year is determined (to the nearest week), and the mean temperature of this period is calculated.
BIO10	Mean temperature of warmest quarter	°C	The warmest quarter of the year is determined (to the nearest week), and the mean temperature of this period is calculated.
BIO11	Mean temperature of coldest quarter	°C	The coldest quarter of the year is determined (to the nearest week), and the mean temperature of this period is calculated.
BIO12	Annual precipitation	mm	The sum of all the monthly precipitation estimates.
BIO13	Precipitation of wettest month	mm	The precipitation of the wettest week or month, depending on the time step.
BIO14	Precipitation of driest month	mm	The precipitation of the driest week or month, depending on the time step.
BIO15	Precipitation seasonality (coefficient of variation)	mm	The coefficient of variation is the standard deviation of the weekly precipitation estimates expressed as a percentage of the mean of those estimates (i.e. the annual mean).
BIO16	Precipitation of wettest quarter	mm	The wettest quarter of the year is determined (to the nearest week), and the total precipitation over this period is calculated.

| CODE	VARIABLE	UNITS	DEFINITION
BIO17	Precipitation of driest quarter	mm	The driest quarter of the year is determined (to the nearest week), and the total precipitation over this period is calculated.
BIO18	Precipitation of warmest quarter	mm	Warmest quarter of the year is determined (to the nearest week), and the total precipitation over this period is calculated.
BIO19	Precipitation of coldest quarter	mm	The coldest quarter of the year is determined (to the nearest week), and the total precipitation over this period is calculated.
Aridity	Global potential aridity	adimensional	Quantify precipitation availability over atmospheric water demand using the ratio between mean annual precipitation and PET
WAI	Water availability index	%	Difference between precipitation and evapotranspiration relative to evapotranspiration (%)
PET	Global potential evapotranspiration	mm	$PET = 0.0023 \times RA \times (Tmean + 17.8) \times TD0.5$, where $Tmean$ is monthly temperature, RA is extra-terrestrial radiation and TD is temperature range.

TABLE S3. Mean, standard error and 95% percentiles [min., max.] for each country of the NFIs used in this study (Spain, Germany, and Finland) for: stand basal area change (SBAc, m^2 ha^{-1} yr^{-1}), basal area growth rate (SBA$_{gain}$, % yr^{-1}), basal area loss rate (SBA$_{loss}$, % yr^{-1}), stand basal area (BA, m^2 ha^{-1}), mean d.b.h. (d$_m$, mm), water availability (WAI, %), minimum temperature (Tmin, ºC), absolute temperature anomaly (TA, ºC) and relative precipitation anomaly (PA, %).

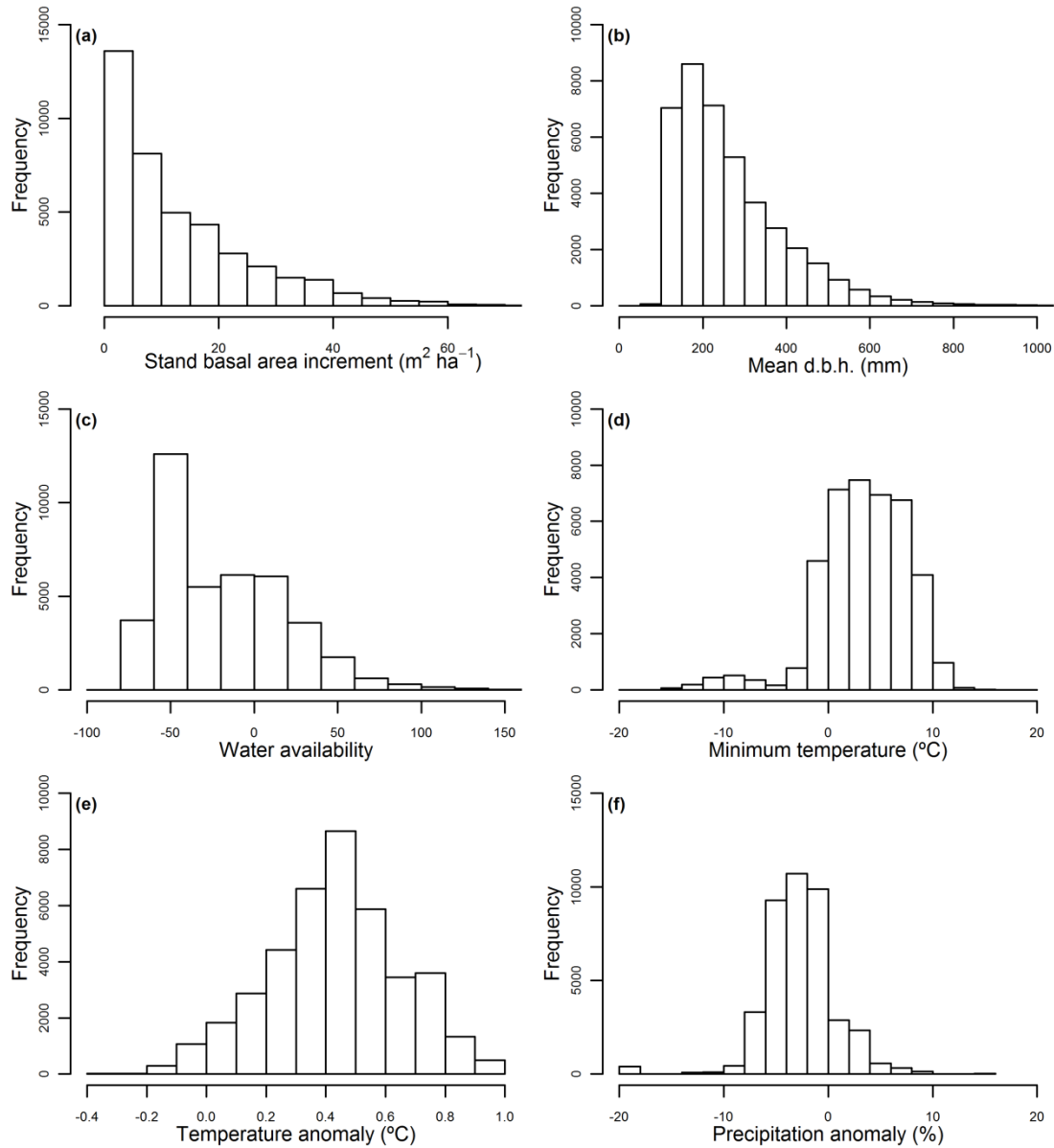|	**Spain**	**Germany**	**Finland**
SBAc (m^2 ha^{-1} yr^{-1})	0.31 ± 0.003 [-0.29, 1.53]	0.83 ± 0.008 [-0.31, 2.57]	0.47 ± 0.009 [-0.05, 1.31]
SBA$_{gain}$ (% yr^{-1})	3.56 ± 0.023 [0.38, 14.29]	4.64 ± 0.054 [0.86, 19.55]	4.31 ± 0.091 [0.60, 13.96]
SBA$_{loss}$ (% yr^{-1})	0.7 ± 0.012 [0.00, 6.86]	0.35 ± 0.014 [0.00, 3.66]	0.21 ± 0.021 [0.00, 2.08]
BA (m^2 ha^{-1})	10.21 ± 0.06 [0.62, 37.57]	24.57 ± 0.16 [4.00, 56.46]	10.07 ± 0.21 [0.34, 29.87]
d$_m$ (mm)	261.84 ± 0.77 [116.00, 601.15]	296.11 ± 1.37 [111.45, 581.65]	165.31 ± 1.19 [106.98, 285.13]
WAI (%)	-30.72 ± 0.19 [-66.84, 54.56]	15.97 ± 0.3 [-18.03, 90.71]	15.69 ± 0.21 [0.55, 30.36]
Tmin (ºC)	5.18 ± 0.16 [-0.10, 10.50]	-0.16 ± 0.13 [-3.20, 2.00]	-9.59 ± 0.57 [-14.60, -5.40]
TA (ºC)	0.55 ± 0.00 [0.30, 0.90]	0.23 ± 0.00 [-0.10, 0.50]	0.1 ± 0.00 [0.00, 0.30]
PA (%)	-3.52 ± 0.02 [-9.09, 1.96]	-0.48 ± 0.03 [-6.67, 4.76]	3.73 ± 0.07 [-2.00, 8.89]

TABLE S4. BIC comparisons of stand basal area change models fitted with non-linear terms or with linear terms for each predictor variable. The full model with non-linear terms included the quadratic term of stand basal area (BA), mean d.b.h. (d_m), water availability (WAI), minimum temperature (Tmin) and precipitation anomaly (PA); and the exponential form for temperature anomaly (TA).

| **REML = FALSE**	**BIC**	**ΔBIC**
WAI linear	57937	0
TA linear	58977	1040
Full model	58988	1051
PA linear	58981	1044
BA linear	58993	1056
Tmin linear	59259	1322
d_m linear	59591	1654
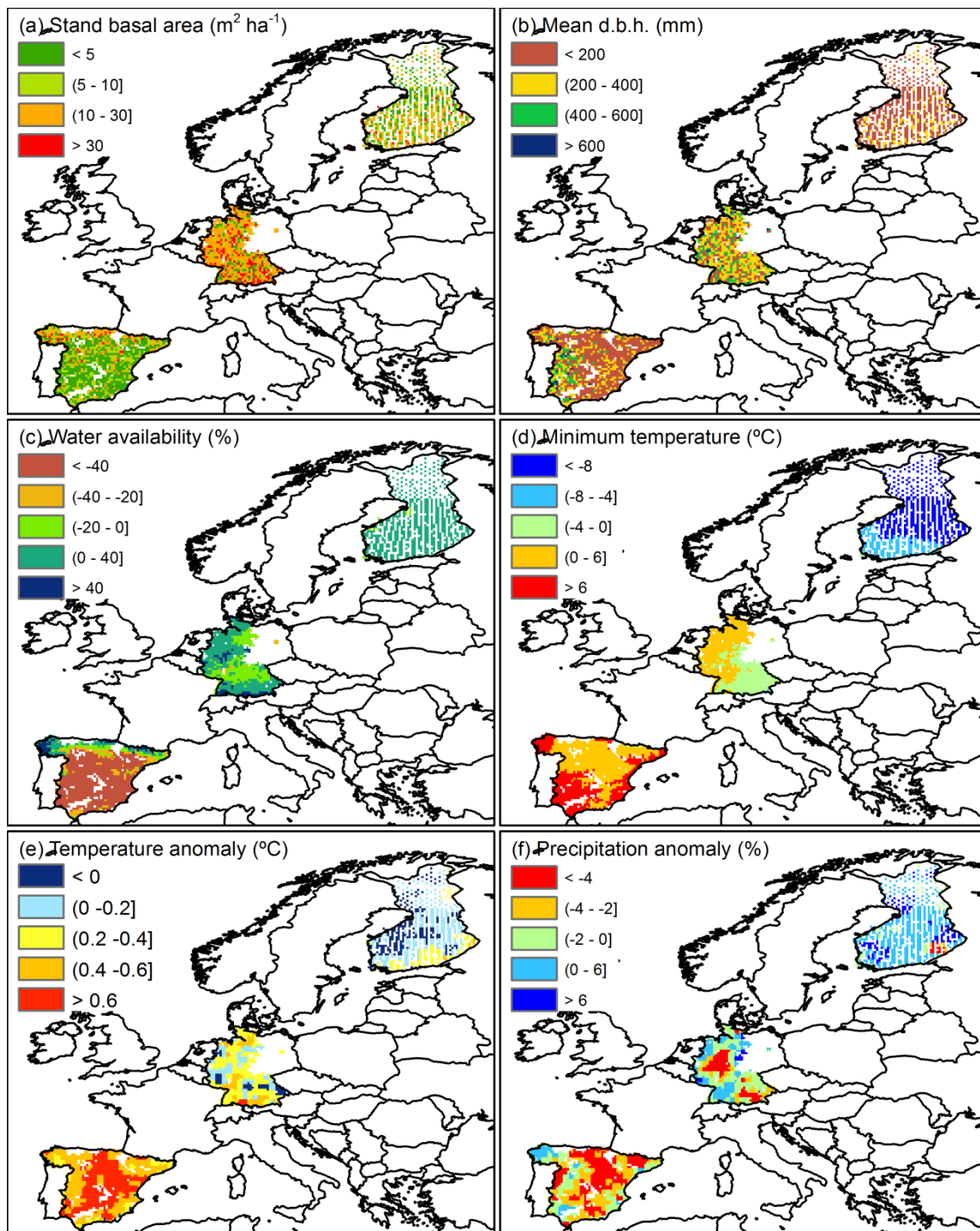
FIGURE S1. Spatial distribution of the predictor variables of stand basal area change in the NFIs included in the study: (a) stand basal area (m^2 ha^{-1}), (b) mean d.b.h. (mm), (c) water availability (%), (d) minimum temperature (ºC), (e) absolute temperature anomaly (ºC), and (f) relative precipitation anomaly (%) in the Spanish, German and Finish NFIs at a spatial resolution of 0.2 x 0.2 degrees.

FIGURE S2. Histograms of the predictor variables of stand basal area change: (a) stand

basal area (m^2 ha^{-1}), (b) mean d.b.h. (mm), (c) water availability (%), (d) minimum

temperature (ºC), (e) temperature anomaly (ºC), and (f) precipitation anomaly (%) in the

Spanish, German and Finish NFIs
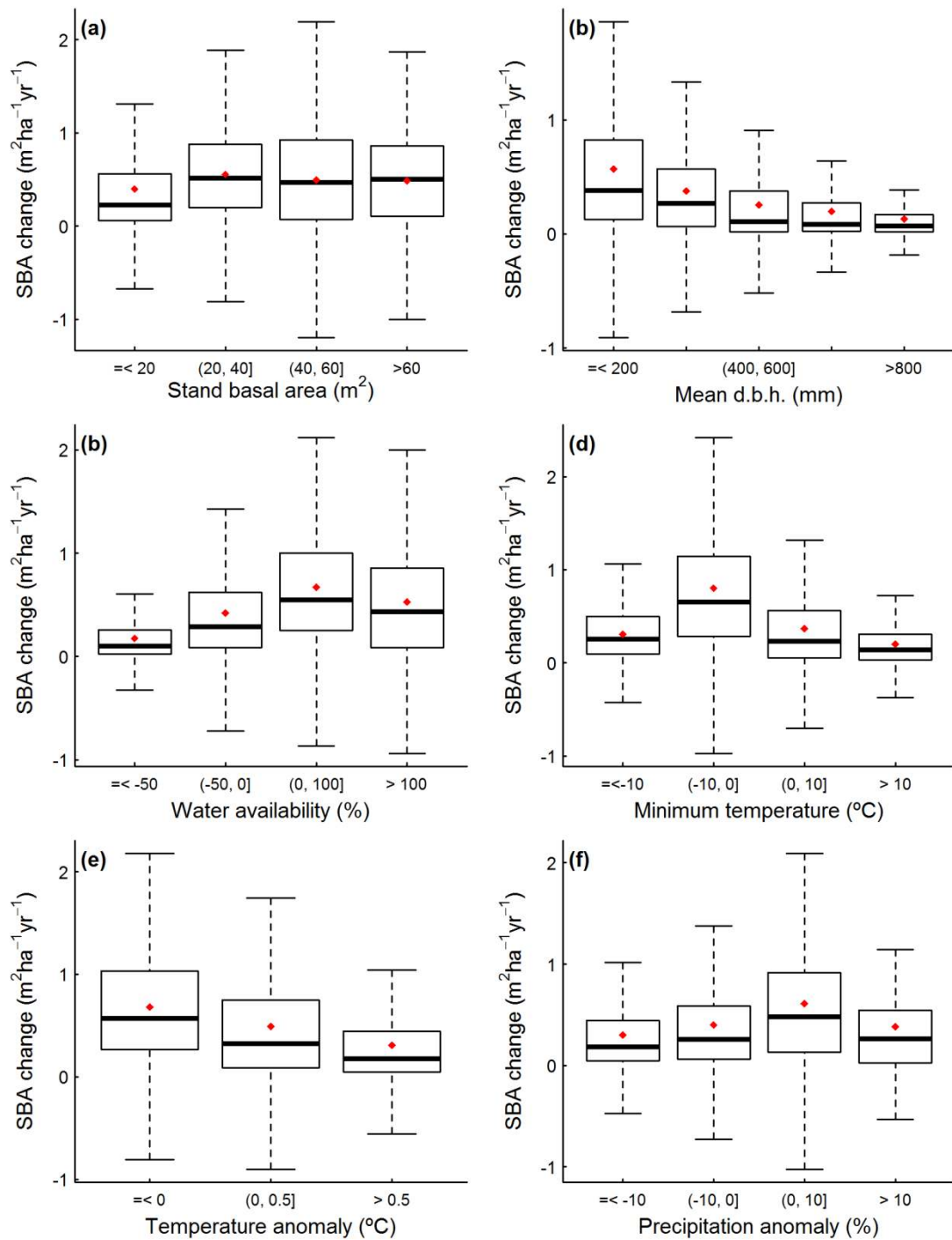
FIGURE S3. Box-whisker plots of stand basal area change (m^2 ha^{-1} yr^{-1}) along (a) stand basal area (m^2 ha^{-1}), (b) mean d.b.h. (mm), (c) water availability (%), (d) minimum temperature (ºC), (e) absolute temperature anomaly (ºC) and (f) relative precipitation anomaly (%).
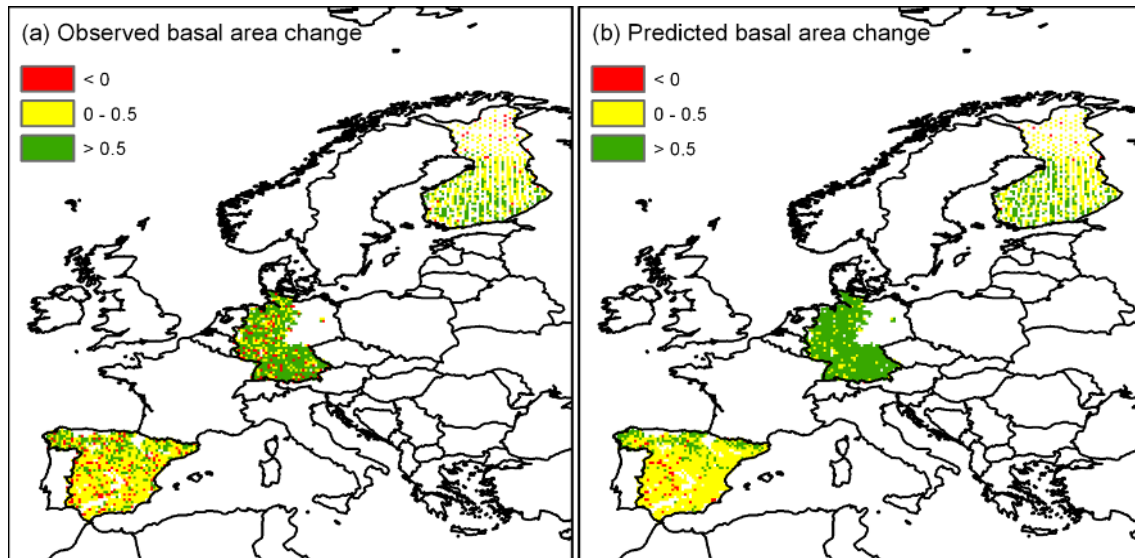
FIGURE S4. Spatial distribution of (a) observed stand basal area change (m^2 ha^{-1} yr^{-1}); and (b) predicted stand basal area change (m^2 ha^{-1} yr^{-1}) in the Spanish, German and Finnish NFIs at a spatial resolution of 0.2 x 0.2 degrees, showing a correlation of 0.9.
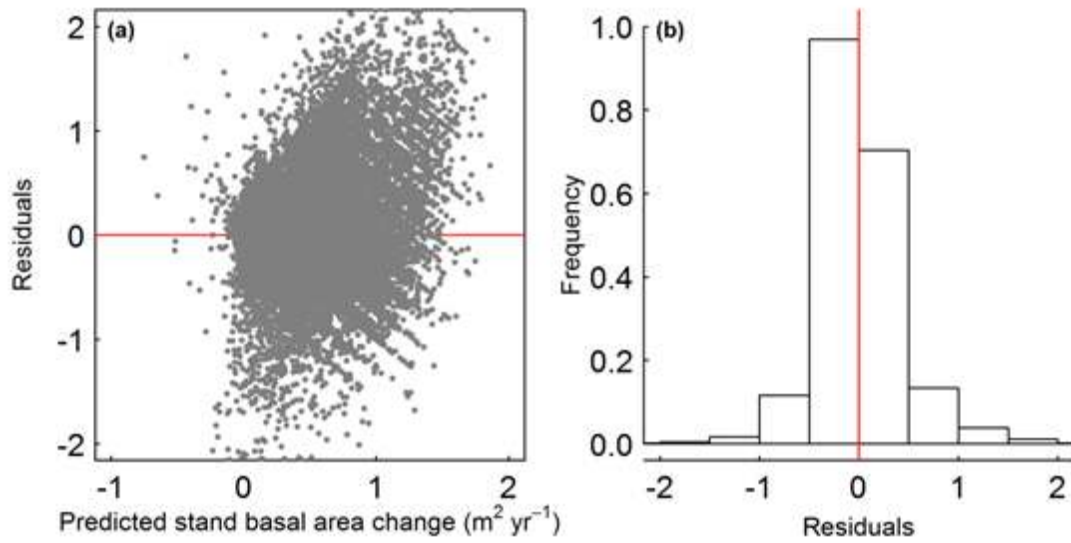
FIGURE S5. Scatterplot of residual versus predicted stand basal area change ((a), m^2 ha^{-1} yr^{-1}) and histogram of the residuals (b) for the best supported model (see Eqn. 1 and parameter values in Table 3).